

Laboratory and field experiments on surface
buoys for current measurement

P.G. Collar and R.M. Carson
Institute of Oceanographic Sciences,
Wormley, Godalming, Surrey,
England.



Introduction

This report summarises some recent work at IOS on the problem of measuring near-surface current in the presence of waves. A fuller account will appear as IOS Report 40. Our main thesis is that it should be possible to measure surface current from a loosely-moored surface-following buoy, and that this measurement will include the Stokes Drift due to locally generated waves; it will thus give a result which is comparable to that of a fully-Lagrangian drifter at the same point. This measurement is no less useful than that of a fixed-point current meter, which measures current without Stokes Drift; and it is a system which may be more easily realised in the open sea than a truly fixed point measurement.

Theory

Using classical small-amplitude wave theory, we have calculated the expected output from a near-surface current meter constrained to move in a variety of geometries. The results are summarised in Table 1. The conclusions are:

- (1) A fixed point current meter does not measure the Stokes Drift

$$S = a^2 \sigma k e^{-2kz_0}$$

where a = wave amplitude

k = wave number

z_0 = mean depth of current meter

$\sigma = 2\pi$ / wave period

- (2) A current meter which is constrained to follow a closed

circular path, which as nearly as possible overlays the actual path of the water particle, and whose axis is maintained horizontal, measures the Stokes Drift exactly.

(3) If the circular path is relaxed to allow the buoy its natural non-circular motion, the Stokes Drift is still measured correctly, to 1st order in ak .

(4) If the constraint is further relaxed, so that the buoy/current meter follows the water surface and the current meter axis is tangential to the wave slope, we still measure Stokes Drift to 1st order ak ; but we do so for a different reason. (Compare \bar{V}_{cm} , \bar{V}_p for the two geometries.)

(5) If we extend the current meter stem below the buoy, to a depth h , we incur an error in measuring Stokes Drift at that depth. However this is such that the measurement can be related, to first order, to the Stokes Drift at the level of the buoy.

(6) The finite buoy diameter is responsible for a high-frequency cut-off in shorter waves: this is significant for wavelengths of less than three buoy diameters; for a buoy of 2m diameter or less, the effect on measured current will be negligible in a typical sea.

We have assumed in these calculations that we possess:

(a) a perfect current meter, which is linear, and measures the component velocity along a chosen axis irrespective of the actual flow vector direction. (i.e. no hydrodynamic stalling).

(b) a perfect mooring which is compliant with respect to wave amplitudes and periods, but which restrains the buoy from drifting over the measuring period.

Wave Tank Experiments

We tested the theory experimentally in the IOS wave tank, using a miniature (3.4cm diameter) electromagnetic (e.m.) current meter to measure the mean drift velocity generated by waves. Dye streaks were used as the absolute reference of velocity - this corresponds to case (6) of Table 1.

The e.m. current meter was mounted on a variety of moorings: the most interesting of these are:

- (a) Fixed point - case (1) Table 1
- (b) Surface following discus) case (4) and (5)
- (c) Surface following catamaran

Results

These are shown as scatter diagrams in Fig. 1 (a) - (c); the main results can be summarised as:

- (a) The fixed spar current meter does indeed fail to measure the contemporary Stokes Drift; the actual measured drift is in the reverse direction.
- (b) The discus buoy is moderately satisfactory if the current meter stem is intermediate in length (9cm). A very long stem introduces errors due to buoy pitching. A very short stem brings the head into a trapped boundary region, about 5cm thick, where the net flow bears no relation to the drift outside. Stalling is not a problem, because flow is generally parallel to the sensor plane.
- (c) The surface following catamaran allows the sensor to be brought very close to a free water surface, while avoiding the boundary region problem. Again a long stem could introduce buoy pitching errors.

Discussion

The results generally bear out the theoretical expectations. In particular the fixed spar (a) and the catamaran (c) demonstrate very clearly the difference between the fixed point Eulerian measurement and the pseudo-Lagrangian buoy measurement. The most important practical conclusion of the tests, however, is the observation that a flat discus buoy traps a surprisingly thick boundary region beneath it. The mechanism appears to be that the buoy, in pitching over the wave crest, captures a volume of water beneath it at the moment when this water might be expected to move on, out from beneath the buoy. This region is thicker than the boundary layer which would

form due to a steady drift shear flow. This is an important consideration in the design of any practical system.

Measurements at Sea

We now attempted to realise a sea-going system in which the sea-surface immediately above the current meter was undisturbed to avoid any boundary layer effect. The general layout is shown in Fig. 2; it is an adaptation of the IOS pitch/roll wave buoy, fitted with an e.m. current meter, and maintained at a depth of 0.5m by three inflated floats. It was coupled to the attendant ship by the usual buoyant wave buoy cable, made compliant by forming a series of catenary loops.

The current meter x and y outputs, sampled at 0.5 s intervals and vector-averaged over 2 minutes, are plotted in Fig. 4 for each of three 20 min. runs. The ship's e.m. log, similarly averaged, is shown for comparison, along with a single vector derived from the path of a free-drifting pinger at 0.5m depth.

In none of the three runs is the agreement between EMPR buoy, pinger and ship's e.m. log good. This is true even for the last series of measurements, made in very calm conditions, in which best agreement might have been expected.

We believe there are several reasons for this:

1. Problems of ship handling, and consequent use of propeller and bow thruster, were causing large variations in the magnitude and direction of flow in the measurement area. Note, for example, the large variations in relative ship position, evident from the ship's e.m. log vectors in Run 3.
2. The uncertainties in estimating pinger velocity and directions were fairly large.
3. The dynamics of the EMPR buoy were manifestly not as good as we had hoped. Considerable improvement should result from:
 - (a) increasing the surface float spacing
 - (b) using a rigid framework in place of the present system of ropes.

4. It is worth stressing that the discrepancies shown in Fig. 4 are actually larger than the expected Stokes Drift component. Thus for Run 2 the Stokes Drift at 0.5m depth is 4.3cm/sec., calculated from the measured unidirectional wave spectrum; while the discrepancy in measured velocity is typically of order 10cm/sec.

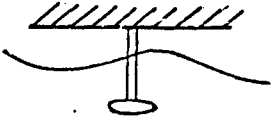
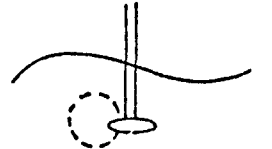

Conclusions

We reiterate our belief that measurement of surface current is best made from a surface following buoy since in this way the contribution from the Stokes component is included with least uncertainty. Some care is required, however, if boundary layer effects are to be avoided underneath a surface follower in very weak currents. Surface current measurements using a surface following buoy deployed from a ship will always risk contamination by the perturbation of flow around the ship's hull. A permanent long term mooring is the next logical development, although we must then face the problem of either reducing the wave and current data in situ, or of telemetering it for subsequent computer processing.

There is a limit to the depth at which useful measurements can be made from a surface follower, but the principle of including the Stokes component applies perfectly well at any depth subjected to wave action. As yet we have not devised a practical solution.


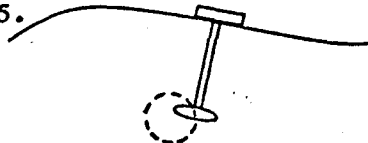

Acknowledgements

We are happy to acknowledge the assistance we have received from C.H. Clayson, V.A. Lawford, A.J. Bunting, G. Griffiths, and J.A. Ewing.

Geometry	Integrated velocity of current meter along axis \bar{V}_{cm}	Integrated particle velocity along axis \bar{V}_p	Integrated current meter output $\bar{V}_p - \bar{V}_{cm}$	Degree of approximation
<p>1.</p>  <p>Fixed point axis horizontal</p>	0	0	0	Exactly
<p>2.</p>  <p>Best-fit circular path. Axis horizontal</p>	0	$a^2 \sigma k e^{-2kz_0}$	$a^2 \sigma k e^{-2kz_0}$	Exactly (cf. Pollard 1973)
<p>3.</p>  <p>Non-circular path, true surface follower: axis horizontal, short stem</p>	0	$a^2 \sigma k e^{-2kz_0}$	$a^2 \sigma k e^{-2kz_0}$	To 1st order in ak

SUMMARY OF RESULTS

TABLE 1 (continued)

Geometry	Integrated velocity of current meter along axis \bar{V}_{cm}	Integrated particle velocity along axis \bar{V}_p	Integrated current meter output $\bar{V}_p - \bar{V}_{cm}$	Degree of approximation
<p>4.</p>  <p>Circular path, short stem, axis parallel to surface/streamline</p>	$-\frac{1}{2} a^2 \sigma k e^{-2kz_0}$	$\frac{1}{2} a^2 \sigma k e^{-2kz_0}$	$a^2 \sigma k e^{-2kz_0}$	<p>To 1st order in ak</p>
<p>5.</p>  <p>Surface follower, long stem h, axis parallel to surface</p>	$-\frac{1}{2} a^2 \sigma k e^{-2kz_0}$	$\frac{1}{2} a^2 \sigma k e^{-2kz_0} \times e^{-kh} (1 + hk)$ $\sim \frac{1}{2} a^2 \sigma k e^{-2kz_0}$	$a^2 \sigma k e^{-2kz_0}$	<p>To 1st order in ak</p>
<p>6.</p>  <p>Lagrangian Drifter</p>	$a^2 \sigma k e^{-2kz_0}$	0	0	<p>Exactly</p>

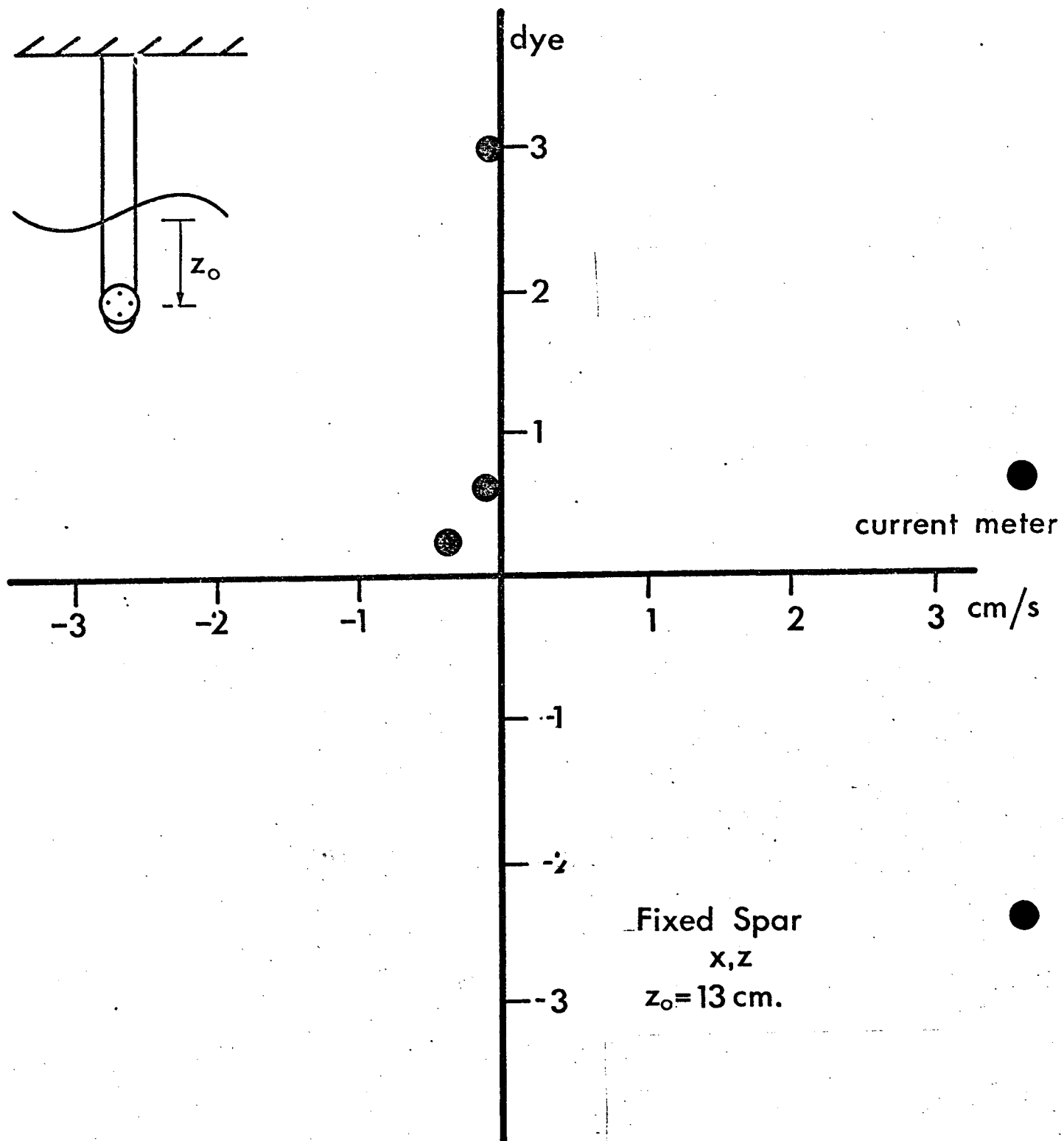


Fig. 1 (a)

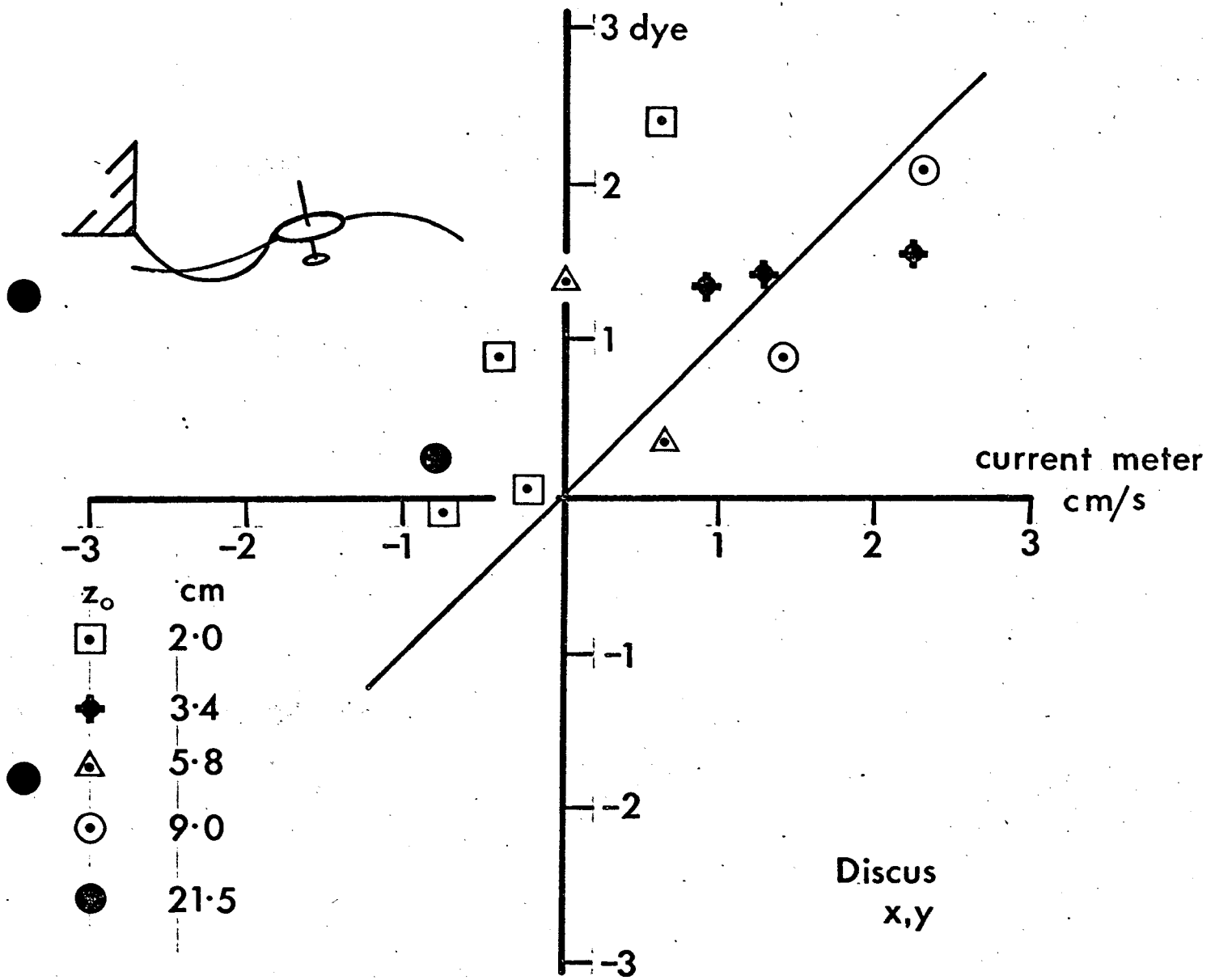


Fig. 1(b)

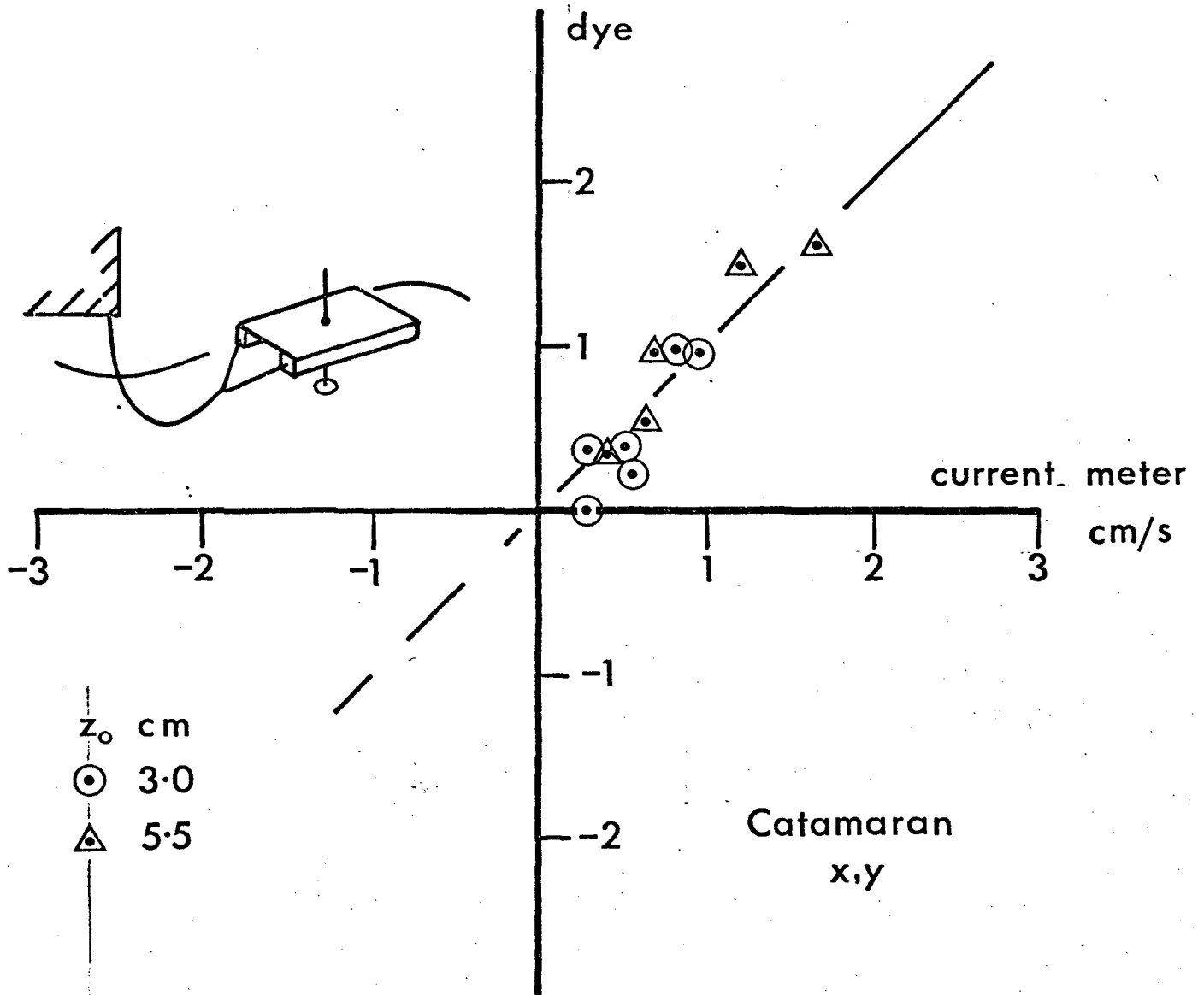


Fig. 1(c)

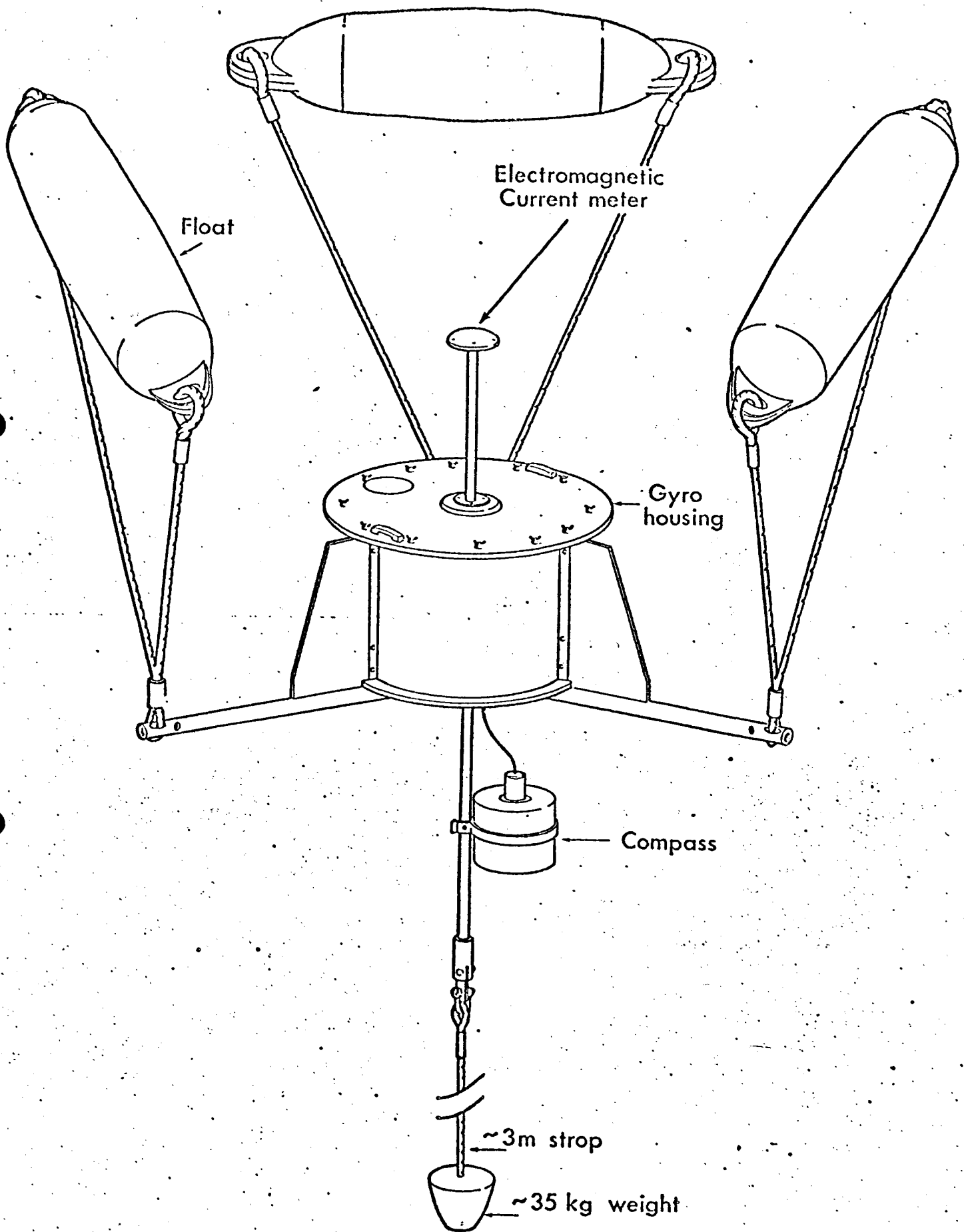
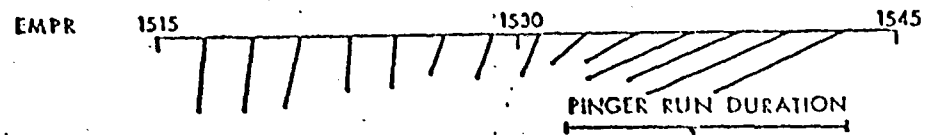
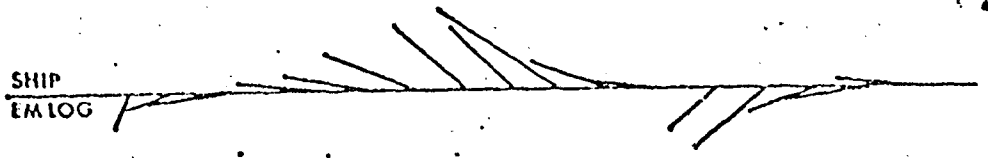


Fig.2 EM PR BUOY



SCALE
20 cm/s

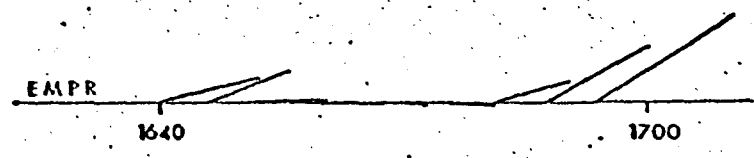
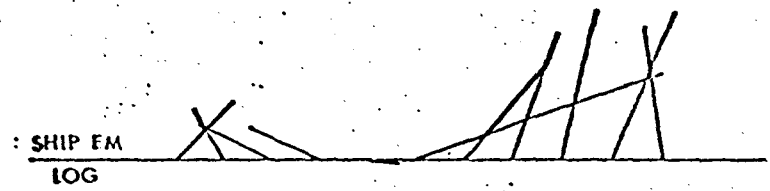
2 mins

PINGER RUN DURATION

WAVE DIR
(wind-o)

PINGER VECTOR

Fig. 4 (a) RUN 2



SCALE
20 cm/s

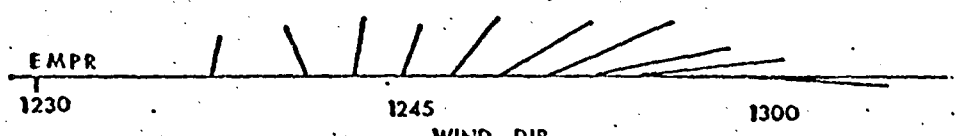
2 mins

PINGER VECTOR

PINGER RUN DURATION

WAVE DIR

Fig. 4 (b) RUN 3



SCALE
20 cm/s

2 mins

WIND DIR

PINGER RUN DURATION

WAVE DIR

PINGER VECTOR

Fig. 4 (c) RUN 4